2023 IEEE/ASME International Conference on Advanced Intelligent Mechatronics (AIM)
June 28-30, 2023. Seattle, Washington, USA

Non-linear Friction Characterisation of the Unwinding Group in a Web Processing Machine

Arul K. Mathivanan, Jasper De Viaene, Yentl Thielemans, Jeroen D. M. De Kooning and Kurt Stockman
Department of Electromechanical, Systems & Metal Engineering, Ghent University, Ghent, Belgium
and *FlandersMake@UGent - Corelab MIRO*, Belgium
Corresponding author: arul.mathivanan@ugent.be

***Abstract*—An experimental methodology is proposed to characterize the friction behaviour of the unwinding group in a web processing machine. The viscous friction effects from the gearbox are of primary focus in this work as they are dominant during the long and steady operating conditions of the web processing machine. The non-linear change in the viscous friction due to the increase in temperature of the gearbox lubricant is experimentally investigated and characterized. Apart from the viscous friction effects from the gearbox, the friction due to the bearings in the unwinding group is also characterised. The experimentally observed friction torque is represented as a 2D map w.r.t to the rotational speed of the motor and the gearbox lubricant temperature. From the obtained results, the non-linear behaviour of the friction is modelled through curve fit method. Also, a viscous friction coefficient derived from the obtained friction measurements is also presented in the work. The proposed methodology can be applied towards developing dynamic models for model-based design applications, control implementation, parameter identification and deployment of digital twins.**

***Index Terms*—Web Processing machine; Non-linear Friction; Parameter Identification; Temperature**

I. Introduction

The manufacturing industry is currently being driven by the demand for efficiency, safety and precision. This has led to a dramatic increase in complexity of manufacturing systems in the past few years. Complexity here is referred to the increase in number of system components, software capacity, measurements and data transfer capabilities [1]. These changes have enabled the identification of complex non-linear system behaviour through the use of models. Friction is one such non-linear behaviour which is present in all mechanical systems which have relative motion and transmit power, e.g. gears or bearings [2]. Although it is a common phenomenon, friction is a major source of power loss in mechanical systems and poses challenges to precise control due its non-linear nature. Web processing applications are also inevitably affected by friction. Web processing machines process web materials such as paper, textile and foils for lamination, coating, slitting, printing, etc. These processes are executed on a web material as it moves through the machine pushed by a series of rollers [3]. Independent roller systems are used to unwind, push and rewind the web material into the machine manipulating the web material speed, tension and stretch as it moves through the machine. Typically a closed loop PI speed control in combination with vector torque control is used to achieve the desired roller speeds. Here, friction can significantly affect the controller performance leading to tracking errors due to its non-linear behaviour [4]. Hence, a good understanding of non-linear friction is beneficial for improving controller performance through feed forward methods. Also, characterising the non-linear friction can be paramount in development and validation of dynamic system models. These accurate models can be deployed in digital twins [5] which can establish predictive maintenance capabilities, control analysis and information to a human operator for safe operation. They also serve as tools in model-based design and development [6].

The types of friction behaviour in rotating components are classified as Stribeck, Coulomb and viscous friction. Stribeck friction is the stick-slip behaviour which occurs during very low speed start-stop conditions [7]. Coulomb friction is the dynamic friction acting as a result of contact between the sliding surfaces. It increases with the load and is reduced through the use of lubrication mediums [8], [9]. In gearboxes, Coulomb friction occurs between the sliding gear faces and is proportional to the torque transmitted [10]. Viscous friction effects are caused by the hydrodynamic resistance due to the surrounding lubrication medium such as gearbox oil and bearing grease [11]. The viscous friction increases proportional to the rotational speed and can be significant in gearboxes due to high rotational speed of gears. These viscous friction losses are also referred to as spin losses and are independent of the load acting through the gearbox. At present, the Lu-Gre [12], Dahl [13] and Bliman-Sorine models [14] are widely used to estimate friction behaviour in dynamic systems. The Lu-Gre model, being the most popular, is extensively used in modern motor control systems for dynamic control [15]. But these models focus predominantly on modelling the stick-slip friction and the hysteresis behaviour of Coulomb friction [16], while the viscous friction is modelled as a linearly proportional value on the rotational speed. As a result, these existing models are more suitable for applications that undergo frequent accelerations and change in directions such as robotic arms or pick-and-place machines, where the Stribeck and load dependant Coulomb friction effects are dominant. But in a web processing application, the rollers are required to operate at steady but significant speeds for long periods under low load conditions. This makes the viscous friction effects more dominant over Stribeck/Coulomb effects. Due to the continuous operation of the rollers for long duration, the churning of the lubricant leads to an increase in the temperature of the lubricant, in-turn affecting its viscosity. This effectively results in changing viscous friction in the gearbox. The above mentioned models do not include the temperature changes on the viscous friction or its non-linear behaviour, which has an influence in web processing machine applications.

Both experimental and model-based analyses have been done in the past to observe the effect of temperature on viscous losses in gearboxes by [11] and [17] respectively. The former modelled the viscous losses in an automotive axle application, which showed a 44% decrease of viscous losses with a 30% increase in lubricant temperature from 50°C - 80°C. The model has been validated on the experimental results obtained by [18]. The latter [17] observed a 0.3 kW decrease in viscous friction power with an increase in lubricant temperature from 20°C to 100°C through a validated physics-based model of a gearbox. That is a 50% decrease in friction with an increase in lubricant temperature of about 80°C. These results confirm the necessity to characterize non-linear viscous friction as a function of temperature. Apart from the gearbox lubricant, there are also viscous friction effects due to the greased bearings, which also are sensitive to temperature. Previous experiments with friction measurements on greased angular contact ball bearings have shown a decrease in bearing friction torque with increasing bearing grease temperature [19]. Reassuringly, the results were consistent for four different types of greases that were used in the study.

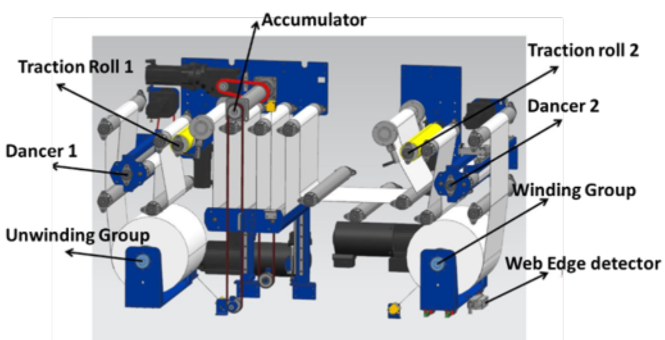

Fig. 1. Experimental Web Processing system.

It is apparent from previous works that the viscous friction is not just dependant on the rotational speed, but also depends on the lubricant temperature. Accurate data on the temperature dependant non-linear viscous friction would be an asset for model validation and to improve control in web processing or similar applications. Therefore, considering temperature as a critical factor, a methodology to characterize the viscous friction in the unwinding part of a web processing machine is presented in this paper. Fig. 1 shows the experimental web processing machine that is used for the friction characterisation. It consists of a winding/unwinding system, dancers, traction rollers and an accumulator, similar to industrial web processing machines. The content of the paper describes the unwinding system, reports on experiments and presents a methodology to characterize the non-linear friction. The characterized friction torque is represented through a 2D map as a function of rotational speed and lubricant temperature.

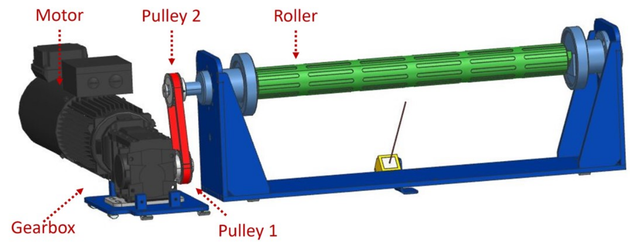

Fig. 2. Unwinding Group of web processing machine.

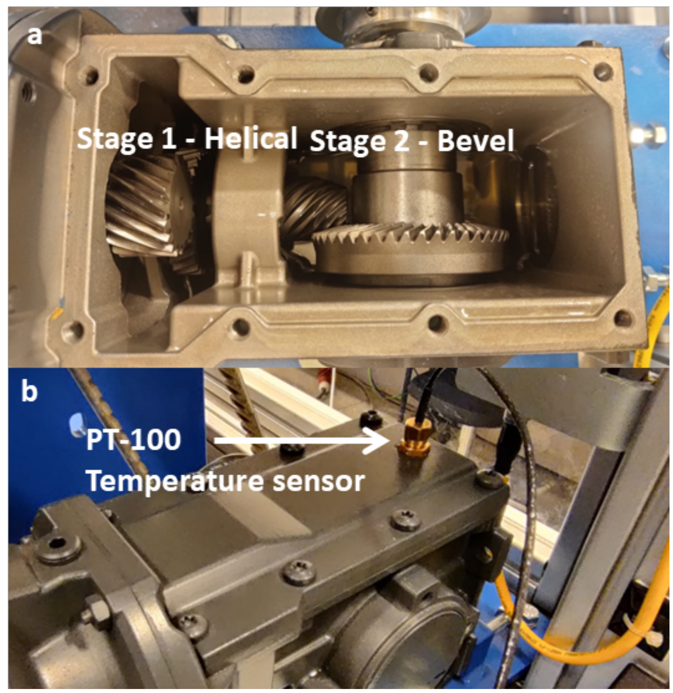

Fig. 3. a) Two stage gearbox. b) PT-100 temperature sensor.

II. System Description

Fig. 2 shows the unwinding group in a web processing machine. It feeds the web material into the machine to be processed using a roller on which the material is wound. The roller is driven by a squirrel cage induction motor that transmits torque to the roller through a two stage gearbox (Fig. 3-a) and a synchronous belt. The two stage gearbox has a helical and a bevel gear stage with a total gear ratio of 6.51. The rated speed of the motor is 1440 RPM. The pulleys are of equal radius resulting in a 1:1 belt transmission ratio.

A Siemens Sinamics G120 drive is used to drive the electric motor controlled by a Siemens Simatic S7 - 1500 PLC. The speed of the system is measured using the integrated motor encoder. The torque from the motor is estimated by the motor controller which uses a PI-based closed loop speed control and vector torque control to achieve the target speed. A PT-100 resistance temperature detector (RTD) is used to measure the gearbox lubricant temperature. The temperature sensor has a thermal response time of 0.1 s, which is sufficiently low to accurately measure the change in temperature. It was mounted through the lubricant fill port as shown in Fig. 3-b. The motor torque, motor speed and lubricant temperature data were logged by the PLC and saved to a MATLAB structure file using an Open Platform Communications United Architecture (OPC UA) interface.

III. Methodology

The unwinding system can be represented as a two mass system, as show in Fig. 4. The first mass is referred to as Mass 1, consists of the motor, gearbox and the driving pulley. The gearbox is part of the lumped mass, and the backlash behaviour has not been considered in the system. The second mass, denoted as Mass 2, consists of the driven pulley and roller. The belt is modelled as a lumped spring damper system.

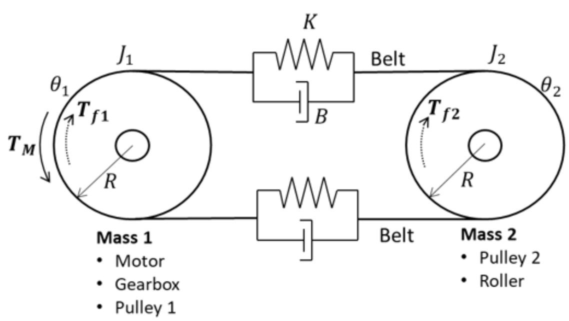

Fig. 4. Two mass model of the unwinding group.

Equations (1) & (2) represent the unwinding system as a dynamic two mass model. The driving torque from the motor is given by T_M. The inertia of the masses 1 & 2 are represented as J_1 & J_2. Similarly, the friction torques of masses 1 & 2 are T_{f1} & T_{f2} respectively. K and B are the stiffness and damping of the belt respectively. Here, θ_1 and θ_2 are the angular displacements of pulleys 1 and 2 respectively. R denote the pulley radius which is the same for both the pulleys 1 & 2.

$$T_M = J_1\ddot{\theta}_1 + T_{f1} + 2R^2\Big[K(\theta_1 - \theta_2) + B(\dot{\theta}_1 - \dot{\theta}_2)\Big] \quad (1)$$

$$0 = J_2\ddot{\theta}_2 + T_{f2} + 2R^2\Big[K(\theta_2 - \theta_1) + B(\dot{\theta}_2 - \dot{\theta}_1)\Big] \quad (2)$$

The motor is taken as the system reference as the speed and torque are measured at the motor shaft. The motor angular displacement θ_M is related to the pulley 1 by (3), where γ is the gearbox ratio.

$$\theta_1 = \gamma\theta_M \quad (3)$$

Generally, viscous friction is modelled proportional to the rotational speed as shown in (4) with a viscous friction coefficient as the proportionality constant.

$$T_f(\dot{\theta}_M) = f\dot{\theta}_M \quad (4)$$

As discussed before, the gearbox in mass 1 causes variable viscous friction effects due to the lubricant which is temperature sensitive. Therefore, friction in mass 1 can be expressed as $T_{f1}(\dot{\theta}_M, t_{GB})$, where t_{GB} denote the gearbox lubricant temperature. The viscous friction coefficient of mass 1 referred to as f_1 can be expressed as a function of lubricant temperature as shown in (5). On the other hand, in mass 2 the bearings are the main source of friction. The bearings exhibit viscous friction behaviour dependant on the rotational speed of the system and can be expressed as in (6). Since a synchronous belt is used, there is no slip and a high transmission efficiency, hence the belt friction can be neglected.

$$T_{f1}(\dot{\theta}_M, t_{GB}) = f_1(t_{GB})\dot{\theta}_M \quad (5)$$

$$T_{f2}(\dot{\theta}_M) = f_2\dot{\theta}_M \quad (6)$$

From (1), which represents the torque balance of mass 1, it can be seen that the torque from the electric motor is used to

1) Accelerate the system - Inertial component
2) Overcome the friction - Friction component
3) Transmit force to the belt - Belt tension component

By removing the belt, mass 1 can be isolated, eliminating the belt tension component and bearing impact due to mass 2. Operating the isolated system at a steady speed eliminates the inertial component resulting in all the transmitted motor torque to overcome the friction of system 1 (T_{f1}). The friction torque is now equal to the torque supplied by the motor which is obtained from the motor controller. The friction of mass 2 can be estimated using the same method but with the belt connected. Now, at a steady speed, the motor torque tries to overcome the friction of the whole system ($T_{fT} = T_{f1} + T_{f2}$). Since the system is operating at steady speed conditions and the center distance between the pulleys is short with high belt stiffness, the belt can be approximated as a rigid power transmission system. The friction of mass 2 can be obtained from the difference between the mass 1 friction and the total friction.

IV. Characterisation of non-linear friction

This section explains the experimental procedure used for characterizing the friction torque as a 2D map dependant on rotational speed of the motor and the lubricant temperature. To obtain the friction torques for different speed and lubricant

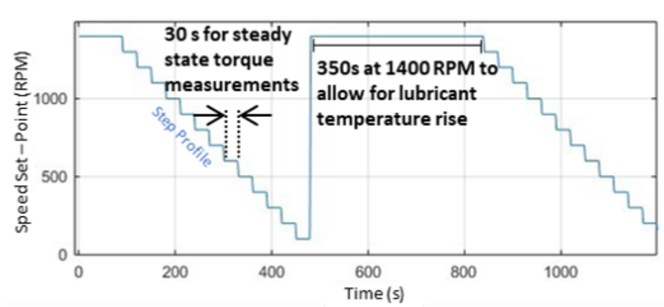

Fig. 5. Motor speed profile used for friction characterisation.

temperatures, the motor is operated over the speed profile shown in Fig. 5. The objective of creating the step-wise profile was to operate the system at different steady state speed conditions and automatically cycle through the required operating points. This allows for measuring the steady state torques at each speed and lubricant temperature. The motor speed is varied between 100 - 1400 RPM in steps of 100 RPM. Each speed is held for 30 s enabling the system to reach steady state. The step-wise speed profile is repeated for multiple cycles with a 6 minute interval in between, to allow for the rise in lubricant temperature. The motor is operated at a speed of 1400 RPM during these intervals. A temperature rise from 19°C to 38°C was observed over the 9500 s duration of the imposed speed profile.

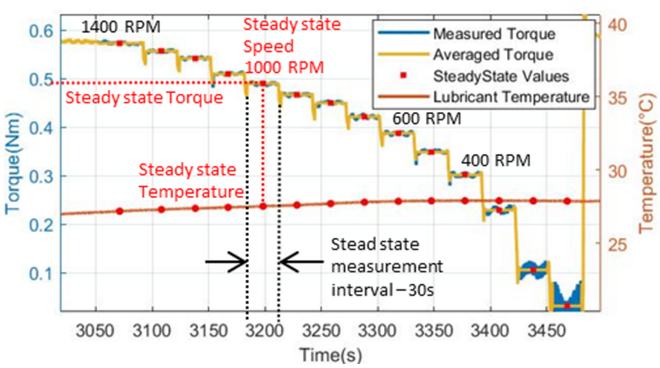

Fig. 6. Obtaining steady state values from experimental data.

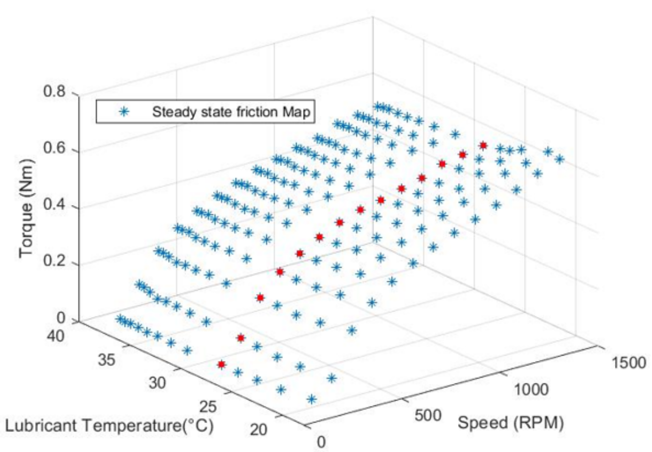

Fig. 7. 2D friction map. Red points show the steady state points from Fig. 6.

Fig. 6. shows a section (3000 - 3500 s) of the measured torques and temperatures for the imposed motor speed profile. It can be observed that the measured torque has fluctuations due to the controller behaviour that can be averaged to obtain the torque at steady state. Similarly, the average temperature over this time is considered. Though the temperature is not entirely steady over the 30 s, the change in temperature is negligible and assumed to not have any significant impact on the friction torque within this time-frame. The steady state torque, speed and temperature values are used to create a 2D map of the friction as shown in Fig. 7. The steady state points highlighted in red correspond to the points shown in Fig. 6.

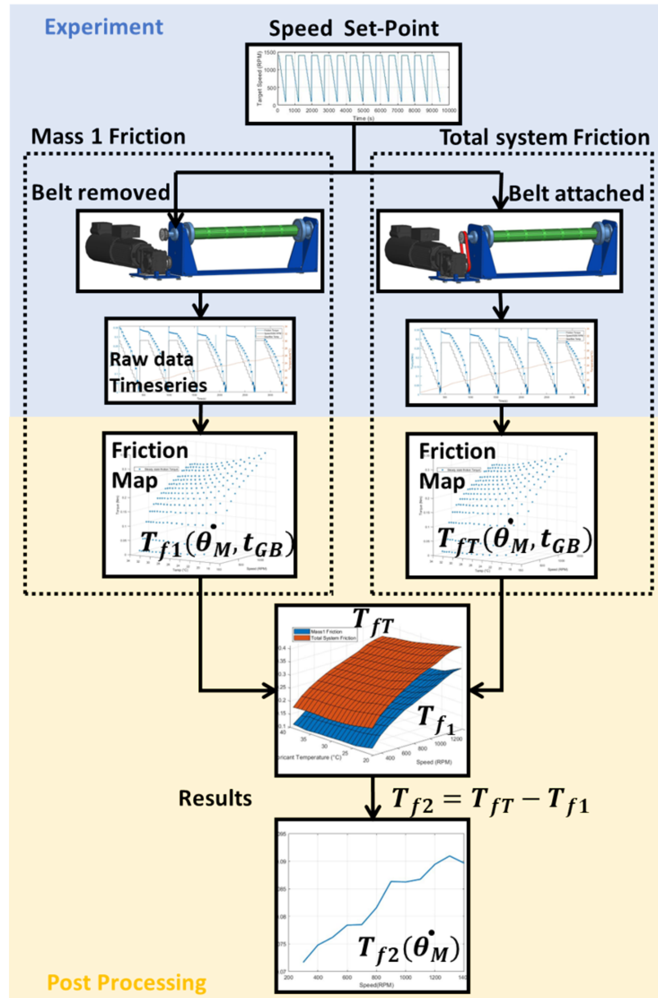

Fig. 8. Friction Characterisation process for unwinding group.

Fig. 8 shows the process flow to characterize the friction. The experiment was carried out with both the belt attached and removed to measure the total system friction and mass 1 (motor and gearbox) friction respectively. Both the friction torques are obtained as a function of motor speed and lubricant temperature. The friction of mass 2 (roller) is obtained by taking the difference between the total (T_{fT}) and mass 1 friction as shown in (7). The effect of temperature on the total system friction is assumed to be only from the gearbox lubricant. Hence, the friction of mass 2 (T_{f2}) is taken to be only dependant on the motor speed.

$$T_{f2}(\dot{\theta}_M) = T_{fT}(\dot{\theta}_M, t_{GB}) - T_{f1}(\dot{\theta}_M, t_{GB}) \tag{7}$$

V. Results and Discussion

From the friction characterisation process in Fig. 8, two sets of experiments were performed to obtain the steady state values. First, to obtain the steady state map of mass 1 (motor and gearbox), and then of the total system. The obtained results were linearly interpolated over a speed - temperature grid with intervals of 100 RPM and 1°C respectively. Fig. 9 shows the map of the friction torques obtained for the mass 1 and total system. It can be observed that the friction from the gearbox is dominant. On average 72% of the total friction in the system is from the mass 1 system (gearbox and motor).

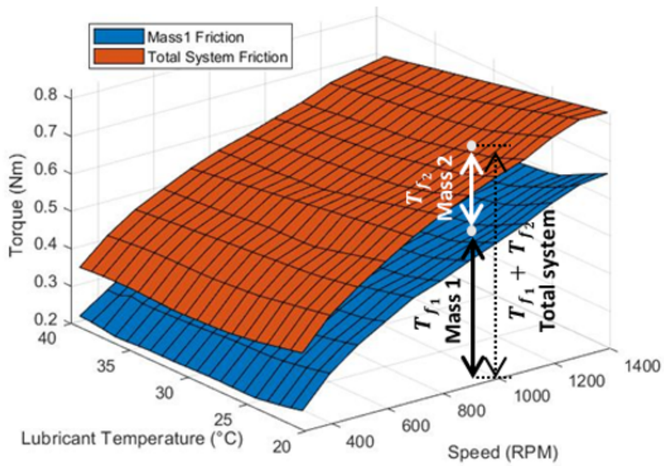

Fig. 9. Comparison of Total system friction and Mass1 (Gearbox) friction.

To observe the viscous friction behaviour due to the gearbox, the friction torque of mass 1 is plotted w.r.t speed for various temperatures, as shown in Fig. 10. It is observed that the friction increases w.r.t motor speed due to the viscous behaviour of the gearbox lubricant. Also, the friction decreases w.r.t to increase in lubricant temperature. A 21% decrease in friction torque is observed when the temperature increases from 20°C and 38°C, especially at speeds greater than 1000 RPM. This is due to the decrease in lubricant viscosity with increase in temperature. From Fig. 10 it can be observed that the drop in friction between 20°C to 23°C is greater compared to the drop in friction between 35°C to 38°C. This shows that the nature of change in friction w.r.t to temperature is non-linear.

It is known from various existing friction models that the viscous friction torque is linearly proportional to the rotational speed [12], [14]. The proportionality is expressed by a constant represented as the viscous friction coefficient f [Nm/RPM], as shown in (3). the experimentally obtained mass 1 friction as shown in Fig 10, can be linearly approximated over the speed to obtain the viscous friction coefficient for each lubricant temperature. The change in the viscous friction coefficient over the lubricant temperature is shown in Fig 11. This resembles a second order polynomial curve which is fitted over the friction coefficient w.r.t temperature curve. The root mean squared error (RMSE) between the fitted curve and experimental values is 1.9%. This is useful to simplify the friction coefficient ($f_1(t_{GB})$) as a function of temperature into an analytical friction model as in (5) which can be integrated into existing friction models. Also the friction coefficient is piece-wisely linear with temperature and can be considered linear within the appropriate temperature boundaries. This is beneficial to include the temperature dependant friction in linear models, e.g. a state space representation.

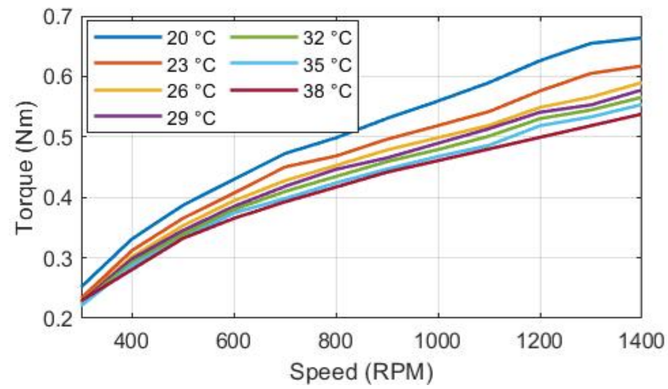

Fig. 10. Viscous friction of the gearbox w.r.t motor speed for various lubricant temperatures.

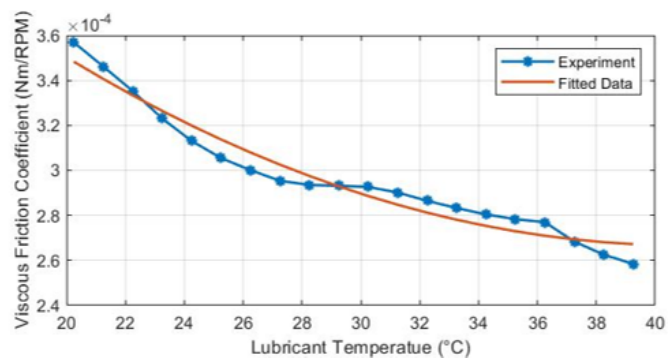

Fig. 11. Viscous friction coefficient(f_1) w.r.t lubricant temperature.

A polynomial curve of higher order can be fitted over the experimentally obtained friction map of mass 1. This polynomial equation provides a more accurate estimation of the viscous friction as shown in Fig. 12. A polynomial equation of 2nd order on speed and 4th order on temperature is fitted over the experimental data. In Fig. 12, the red points represent the fitted torque as compared to the experimentally obtained friction torque shown by the black points and the blue surface. The RMSE of the fitted surface compared to the experimentally obtained friction values is 1.8%.

As the total friction and mass 1 friction is now known, the friction of mass 2 due to the roller bearings is calculated using (7). The variation of mass 2 friction (T_{f2}) is considered only due to increase in rotational speed as in (6). Fig. 13 shows the friction of mass 2. It can be observed that the viscous friction increases with increase in rotational speed. The trend looks linear as observed by a fitted line over the experimental data in Fig. 13. From the linear approximation, the viscous friction coefficient of mass 2 (f_2) as in (6) is obtained.

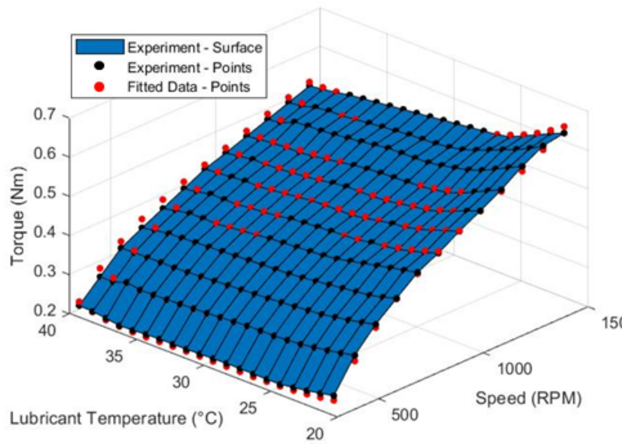

Fig. 12. Mass 1 friction (T_{f1}) represented by a higher order polynomial surface.

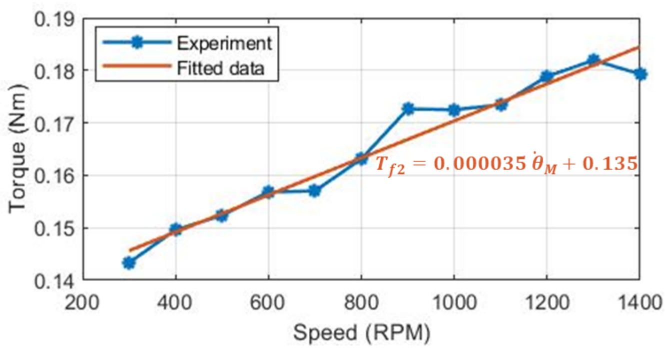

Fig. 13. Bearing friction in mass 2 (T_{f2}) w.r.t motor speed.

VI. Conclusion

The proposed methodology is successful in characterizing the viscous friction behaviour in unwinding group of the web processing machine. The non-linear viscous friction behaviour and the effect of lubricant temperature is experimentally observed and presented through the results. The methodology can be applied to other similar applications that use drives coupled with gearboxes. It is suitable for long duration, high speed and low load operations where the temperature dependant viscous friction effects are dominant. Also, the method enables to identify the temperature dependant viscous friction coefficient f, which can be integrated into physics-based dynamic models. These models are suitable for use in adaptive feed forward control and to estimate the non-linear friction behaviour for faster response and elimination of overshoot. Future research will focus on developing an online friction estimation model to be deployed as a digital twin of the web processing machine. In the future, the characterized friction model presented in this paper will serve as the benchmark for validating an online friction estimation method. Also, by comparing the online friction estimation with the characterized friction model, anomalies can be detected in the gearbox and bearings of the unwinding group for condition monitoring purposes.

Acknowledgment

This research is supported by the Flanders Make CADAIVision SBO project. The authors would like to thank the Flemish Government for funding this research.

References

[1] W. Dieterle, "Mechatronic systems: Industrial applications and modern design methodologies," *IFAC Proceedings Volumes*, vol. 37, no. 14, pp. 1–5, 2004. 3rd IFAC Symposium on Mechatronic Systems 2004, Sydney, Australia, 6-8 September, 2004.

[2] G. Abba and P. Sardain, "Modeling of frictions in the transmission elements of a robot axis for its identification," *IFAC Proceedings Volumes*, vol. 38, no. 1, pp. 7–12, 2005. 16th IFAC World Congress.

[3] P. Pagilla, N. Siraskar, and V. R. Dwivedula, "Decentralized control of web processing lines," *Control Systems Technology, IEEE Transactions on*, vol. 15, pp. 106 – 117, 01 2007.

[4] Hu Hongjie, Wang Yuanzhe and Sun, Guowei, "Hybrid adaptive compensation control scheme for high-precision servo system," *Transactions of Tianjin University*, vol. 19, pp. 217–224, June 2013.

[5] E. VanDerHorn and S. Mahadevan, "Digital twin: Generalization, characterization and implementation," *Decision Support Systems*, vol. 145, p. 113524, 2021.

[6] C. F. Barbieri, Giacomo and R. Borsari, "A model-based design methodology for the development of mechatronic systems.," *Mechatronics*, vol. 24, p. 833–843, 2014.

[7] B. Zhang, Y.-l. Dong, K.-d. Zhao, and G.-q. Li, "Study on the friction nonlinear control of force control system," in *2007 International Conference on Mechatronics and Automation*, pp. 3695–3699, 2007.

[8] M. Akbari, M. A. Badamchizadeh, and M. Poor, "Implementation of a fuzzy tsk controller for a flexible joint robot," *Discrete Dynamics in Nature and Society*, vol. 2012, 10 2012.

[9] K. Michaelis, B.-R. Hoehn, and M. Hinterstoißer, "Influence factors on gearbox power loss," *Industrial Lubrication and Tribology*, vol. 63, pp. 46–55, February 2011.

[10] P. Q. Carlos Wilfrido, A. Gabriel, A. Jean-Francois, R. Thibaut and G. Philippe, "Load-dependent Friction Laws of Three Models of Harmonic Drive Gearboxes Identified by Using a Force Transfer Diagram," *International Conference on Mechanical and Aerospace Engineering*, pp. 239–244, July 2021.

[11] D. Talbot, A. Kahraman, S. Li, A. Singh, and H. Xu, "Development and validation of an automotive axle power loss model," *Tribology Transactions*, vol. 59, no. 4, pp. 707–719, 2016.

[12] K. Johanastrom and C. Canudas-de Wit, "Revisiting the lugre friction model," *IEEE Control Systems Magazine*, vol. 28, no. 6, pp. 101–114, 2008.

[13] C. Canudas de Wit, H. Olsson, K. Astrom, and P. Lischinsky, "A new model for control of systems with friction," *IEEE Transactions on Automatic Control*, vol. 40, no. 3, pp. 419–425, 1995.

[14] P.-A. Bliman, "Friction modelling by hysteresis operators: application to dahl, sticktion and stribeck effects," in *Proc. Conf. on Models of Hysteresis, Trento, 1991*, 1991.

[15] X. Wang, S. Lin, and S. Wang, "Dynamic friction parameter identification method with lugre model for direct-drive rotary torque motor," *Mathematical Problems in Engineering*, vol. 2016, March 2016.

[16] de Wit, Carlos Canudas and Olsson, Henrik and Åström, Karl Johan and Gäfvert, Magnus and Lischinsky, Pablo, "Friction Models and Friction Compensation," *European Journal of Control*, vol. 4, no. 3, 1998.

[17] S. Seetharaman and A. Kahraman, "Load-Independent Spin Power Losses of a Spur Gear Pair: Model Formulation," *Journal of Tribology*, vol. 131, February 2009.

[18] H. Xu, A. Singh, A. Kahraman, J. Hurley, and S. Shon, "Effects of Bearing Preload, Oil Volume, and Operating Temperature on Axle Power Losses," *Journal of Mechanical Design*, vol. 134, April 2012.

[19] da Silva, Levi N. Tessari, Kerolin F. Privatti, Mário W. Wagner, Alfons R. and Aurichio, Thiago, "Torque-Speed-Temperature Relationship in Grease Lubricated Angular Contact Ball Bearings," *SAE Technical Paper*, September 2015.